Turk J Chem
35 (2011) , 37 – 44.

doi:10.3906/kim-0912-434

Effect of CMC and HPC mixture on the photocatalytic activity of Nd-TiO_2/SiO_2 film under visible light irradiation

Parviz ABEROOMAND AZAR[1], Shahram MORADI DEHAGHI[2], Susan SAMADI[1,*], Mohammad SABER TEHRANI[1] and Mohammad Hadi GIVIANRAD[1]

[1] *Department of Chemistry, Science and Research Branch, Islamic Azad University, P.O. Box 14515-775, Tehran-IRAN*

e-mail: susansamadi@iausr.ac.ir

[2] *Faculty of Chemistry, Tehran North Branch, Islamic Azad University, Tehran-IRAN*

Received 31.12.2009

Neodymium-titania/silica films were prepared by the sol-gel method with the addition of various amounts of hydroxy propyl cellulose (HPC) and 5.09 $\times$ 10^{-5} g $g^{-1}_{solution}$ of carboxy methyl cellulose (CMC) in saturated conditions. The porous Nd-TiO_2/SiO_2 was obtained after heat treatment for 2 h at 500 °C, with the surface area up to 276 m^2 g^{-1}, which was measured using the Brunauer, Emmett, and Teller (BET) method. Scanning electron microscopy (SEM) showed that the particle size of Nd-TiO_2/SiO_2 decreased and the microstructure of the film became loose in suitable conditions with the addition of CMC to HPC. Subsequently, the photocatalytic activity of Nd-TiO_2/SiO_2 film under visible light irradiation was achieved to an optimum when the concentrations became 3.825 $\times$ 10^{-3} and 5.09 $\times$ 10^{-5} g $g^{-1}_{sol.}$ for HPC and CMC, respectively.

Key Words: Self-cleaning, sol-gel, photocatalysis, nanocomposite

Introduction

Mesoporous titania materials have attracted the worldwide attention of researchers due to their extraordinary optical properties, electrical properties, easy methods of synthesis, and good chemical stability.[1−3] Recently,

*Corresponding author

the application of semiconductor heterogeneous photocatalysts, especially titania, in the photodegradation of toxic organic pollutants has been extensively investigated.[4] The activity of the TiO_2 catalyst depends on its crystal structure, morphology, surface area, and porosity, as well as the shape and distribution of pores.[5] It has been revealed that anatase and nanosized TiO_2 particles with porous structures showed better photocatalytic activity.[6,7]

HPC is a well-known dispersant used for preventing agglomeration of titania powder. In recent years, there has been a growing interest in the use of thin, transparent TiO_2 film for generating a self-cleaning surface. HPC is therefore used to prepare mesoporous TiO_2 thin films.[8] CMC and HPC are very similar in structure; therefore, CMC was selected with HPC as additives.

Due to the large band gap (E_{bg} of approximately 3.2 eV), all photon-driven applications of TiO_2 require ultraviolet light for excitation. Band gap tailoring by doping is the most efficient and frequently used approach. Doping, within certain limits, serves to prolong the lifetime of charge carriers if the dopants have energy levels just below the conduction band or just above the valence band of titania to realize shallow charge carrier trapping. Band gap narrowing also becomes possible if the electronic coupling effect between the dopant and semiconductor is strong enough to change the structure of the band.[9] Doping with various metal ions, such as Mn[10], V[11–14], Fe[15–17], Cr[11], Zr[18], Cu[19], and Nd[8,9,20–22], has been attempted in order to improve the photocatalytic activity and to shift the optical absorption of TiO_2 to the visible region (red shift).

It has been observed that the addition of SiO_2 to TiO_2 films not only permits an increase of in-time persistence of the photoinduced superhydrophilicity,[23–25] but also creates an extremely large surface area.[26] An optimal persistence of the natural superhydrophilicity was observed for a nanocomposite film with a molar composition of a 60:40 ratio of TiO_2 and SiO_2, deposited from a TiO_2 anatase crystalline suspension and a SiO_2 polymeric sol and subsequently heat-treated for 2 h at 500 °C.[27]

In the present work, HPC and CMC were introduced to prepare nanosized Nd-TiO_2/SiO_2 composite films by the sol-gel method.

Experimental

Materials

Titanium tetraisopropoxide (TTIP) and neodymium nitrate (both AR analytical grade, Merck Chemical Company) were used as titanium and neodymium sources for the preparation of the Nd-TiO_2 phtocatalysts. HPC, CMC, HNO_3, SiO_2 colloid solution, and absolute ethanol were purchased from Merck. The reagents used for the preparation of all solutions were of the highest obtainable purity, using deionized water in the NANOpure water system with a specific resistivity of 18.3 MΩ cm^{-1} (Millipore).

Characterizations

The microstructure of the film samples was observed with an XL30 scanning electron microscope (SEM). The specific surface area of powder was measured with a Model JW-K surface area analyzer (Beijing JWGB Sci. & Tech. Co.). The phase composition of the powders was determined with a SCIFERT-3003 PTS X-ray diffractometer. The FT-IR analysis was carried out for the samples with a Thermo Nicolet NEXUS-870.

Photocatalytic properties of the films were investigated by measuring the optical absorption of a methyl orange solution, 10 ppm, before and after the photodegradation with a Varian UV-Vis spectrophotometer. The photocatalytic activities were studied at the absorption peak (465 nm) before and after the photodegradation.

Preparation of samples

The solutions were prepared based on the method of Zhao et al.,[8] and the only difference was the addition of SiO_2 to the solution. The 5 types of Nd-TiO_2/SiO_2 photocatalyst films were prepared by using the sol-gel method. TTIP was dissolved in absolute ethanol with various amounts of HPC and 5.09×10^{-5} g $g_{sol.}^{-1}$ of CMC with a 1:125 molar ratio of TTIP to ethanol, then stirred until complete dissolution (Table). Afterwards, another mixture of absolute ethanol, HNO_3, deionized water, SiO_2, and $Nd(NO_3)_3$, with a molar ratio of ethanol/HNO_3/H_2O/$Nd(NO_3)_3$/SiO_2 = 43:0.2:1:0.002:0.40, was added dropwise with vigorous stirring. The obtained transparent colloidal suspension was stirred for 30 min and then aged for 48 h, until it formed as a gel. Finally, the tiles were coated by a dip-coating method after pretreatment with fluoric acid.

Table. Formulation and characterization of sample sol-gel.

Sample	Amount of HPC in solution, g $g_{Sol.}^{-1}$	Amount of CMC in solution, g $g_{Sol.}^{-1}$	Surface area, m^2 g^{-1}	Decomposition time of methyl orange, h
1	4.5×10^{-3}	-	331.76	4.50
2	4.275×10^{-3}	5.09×10^{-5}	250.37	4.25
3	4.05×10^{-3}	5.09×10^{-5}	263.5	4.00
4	3.825×10^{-3}	5.09×10^{-5}	276.67	3.25
5	3.6×10^{-3}	5.09×10^{-5}	187.63	4.00

Photocatalysis

The solution of methyl orange in deionized water, with a concentration of 10 ppm, was chosen as a matter of photodegradation. This solution was set in the vicinity of the tiles under a 400 W high-pressure mercury vapor lamp (Osram). The spectrum of this lamp is shown in Figure 1. As can be seen there, a large amount of the radiation was located in the visible region. The concentration changes of the methyl orange were determined by a UV-Vis spectrophotometer. The methyl orange solution was placed in the vicinity of the tiles for 12 h in the darkness for elimination of adsorption of the solution to the surface of the catalyst (Figure 1).

Results and discussion

The effect of CMC and HPC on the microstructure

The FT-IR spectra of the powders with various amounts of HPC and 5.09×10^{-5} g $g_{sol.}^{-1}$ of CMC are shown in Figure 2, in a wave number range of 4000-400 cm^{-1}. The bands at 3000-3700 cm^{-1} should be assigned to

the symmetric vibration of a surface hydroxyl group.[8,21,28,29] A large amount of propanol appeared during the hydrolysis of TTIP, which led to the appearance of hydroxyl bands (3100-3700 cm^{-1}). The absorption bands around 1630 cm^{-1} were assigned to H-O-H bending physically adsorbed water and the hydroxyl group.[21] The band at 618 cm^{-1} corresponded to the Ti-O-Ti stretching motion.[8,30] The absorption peak at 1081 cm^{-1} was the asymmetrical vibration of the Si-O-Si bond in the tetrahedral SiO_4 unit of the SiO_2 matrix.[31] The symmetrical Si-O-Si stretching vibration appeared at 791 cm^{-1}, along with a peak at 950 cm^{-1}; this band was ascribed to the vibration involving a SiO_4 tetrahedron bonded to a titanium atom through Si-O-Ti bonds.[31] Consequently, the presence of this band confirmed the presence of Si-O-Ti linkages in the Nd-TiO_2/SiO_2 nanocomposite product. The peak at 480 cm^{-1} was due to the vibration modes of anatase skeletal O-Ti-O-Nd bonds (Figure 2).[21]

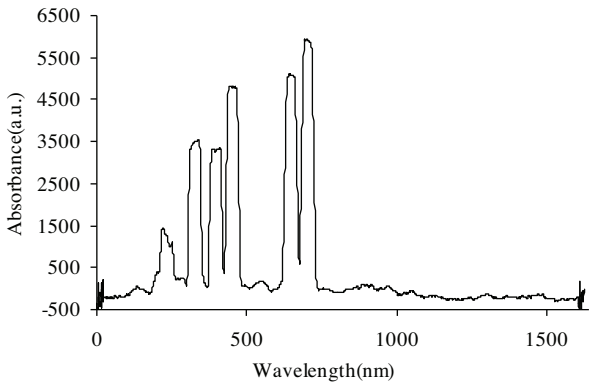

Figure 1. Spectrum of high-pressure mercury vapor lamp.

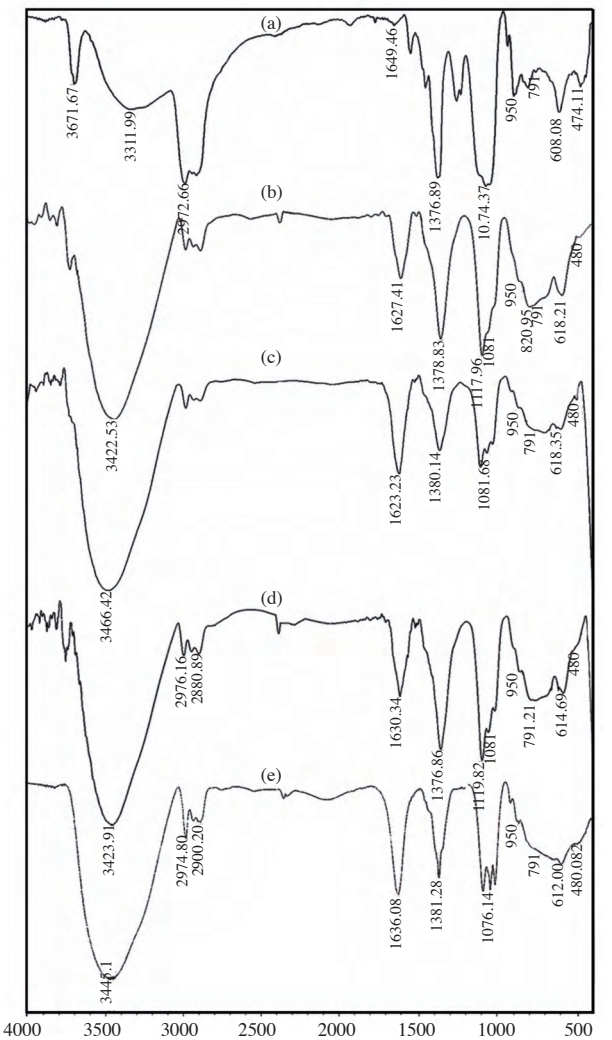

Figure 2. The FT-IR spectra of the sol-gel with various amounts of HPC and CMC additives:. (a) Sample 1, (b) Sample 2, (c) Sample 3, (d) Sample 4, (e) Sample 5.

The SEM images are presented in Figure 3. When HPC was decreased from 4.5×10^{-3} to 3.825×10^{-3} g $g_{sol.}^{-1}$ with 5.09×10^{-5} g $g_{sol.}^{-1}$ of CMC, the Nd-TiO_2/SiO_2 particle size decreased, and its distribution became narrow in suitable conditions (see Figure 2, Samples 1-4). Nevertheless, when the amount of HPC was 3.6×10^{-3} g $g_{sol.}^{-1}$ with saturated CMC (Sample 5), the particle size of the sample film increased. Accordingly, the agglomeration of Nd-TiO_2/SiO_2 particles decreased and the film became porous when CMC was added to HPC. Sample 4 with HPC (3.6×10^{-3} g $g_{sol.}^{-1}$) and CMC (5.09×10^{-5} g $g_{sol.}^{-1}$) had the most uniform particle distribution with low agglomeration and a porous microstructure (Figure 3).

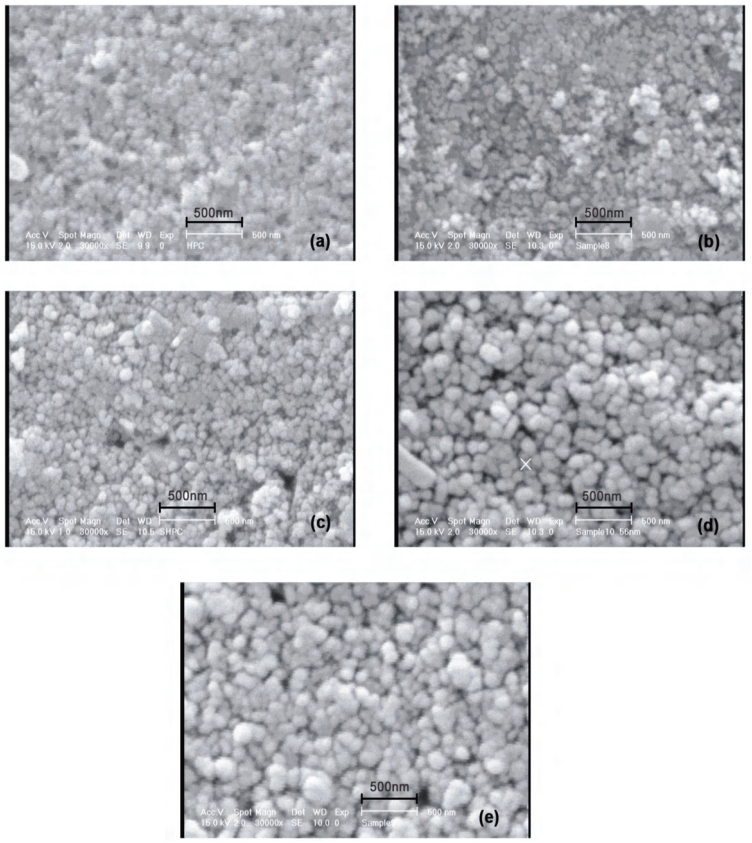

Figure 3. SEM images for the sample films: (a) Sample 1, (b) Sample 2, (c) Sample 3, (d) Sample 4, (e) Sample 5.

The effects of CMC and HPC on the anatase phase

XRD patterns of 5 samples are shown in Figure 4. The XRD measurements revealed that the samples possessed an anatase structure, and evidence of rutile and mixed phases was not observed. The samples presented different proportions of anatase phase. According to Figure 4, Sample 4 was fully crystalline and was only in the anatase form. It was in good shape for self-cleaning ability. It can be deduced that the addition of CMC to HPC facilitated the formation of the anatase phase at a temperature of 500 °C (Figure 4).

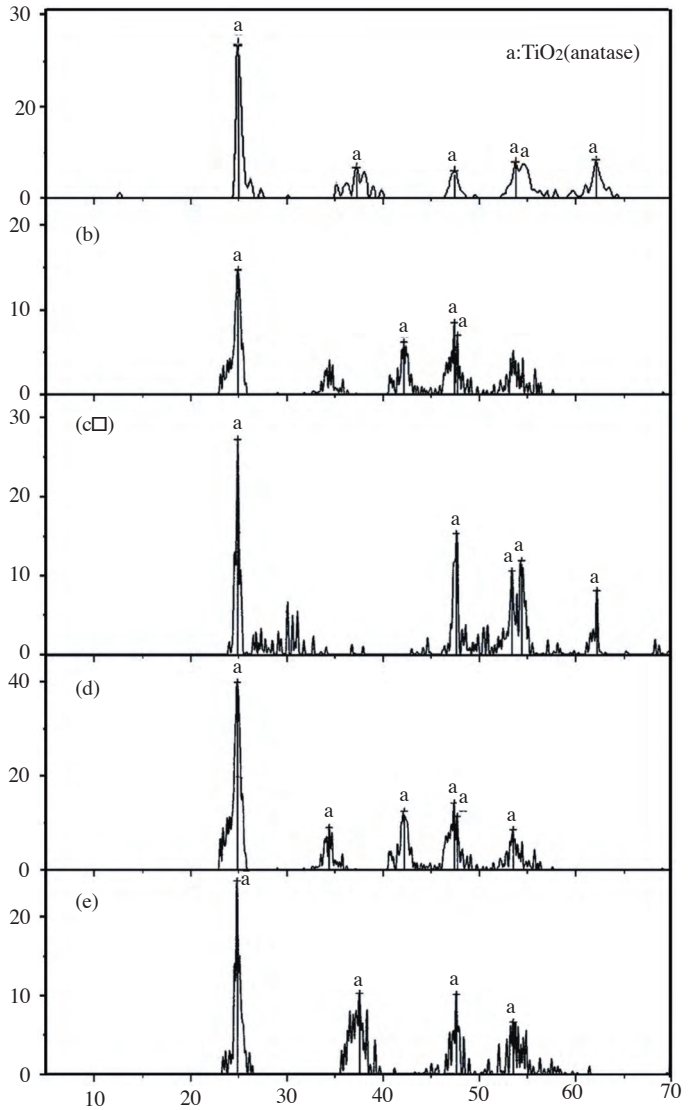

Figure 4. XRD patterns of sol-gel synthesized Nd- TiO_2/SiO_2: (a) Sample 1, (b) Sample 2, (c) Sample 3, (d) Sample 4, (e) Sample 5.

The effects of CMC and HPC on the self-cleaning ability

The Table shows the relationship between the amount of HPC with CMC and the photocatalytic activity of the samples. The decomposition time of methyl orange in the visible light region decreased when the percentage of HPC in the presence of CMC decreased (Samples 1-4). Moreover, it was found that the photocatalytic activity would be improved by the addition of CMC to a certain amount of HPC. The values of the surface area of sample films are listed in the Table. As tabulated, Sample 1 had the highest amount of BET, the lowest particle sizes of Nd-TiO_2/SiO_2, and the longest period for the decomposition of methyl orange. It might be inferred that when Nd-TiO_2/SiO_2 particle size decreases, the self-cleaning ability would increase, but there is

a limitation for the decrease of particle sizes. If particle size decreases beyond this limit, self-cleaning ability would decrease. The relationship between the amount of HPC with CMC and the photocatalytic activity of the samples could be explained by the evolution of the microstructure of the film samples. The Nd-TiO_2/SiO_2 film becomes porous and the particle size decreases in suitable conditions when CMC is added to a certain amount of HPC. Consequently, the active site number should be greater due to the increasing of the surface area. Therefore, the good self-cleaning ability of Sample 4 under visible light should be ascribed to the suitable porous and agglomerated microstructure (Table).

Acknowledgment

The authors are very grateful to the Laboratory Complex of IAU for valuable technical assistance.

References

1. Agarwala, S.; Ho, G. W. *Mater. Lett.* **2009**, *63*, 1624-1627.
2. Li, H.; Wang, J.; Li, H.; Yin, S.; Sato, T. *Mater. Lett.* **2009**, *63*, 1583-1585.
3. Ohno, T.; Numakura, K.; Itoh, H.; Suzuki, H.; Matsuda, T. *Mater. Lett.* **2009**, *63*, 1737-1739.
4. Hafez, H. S. *Mater. Lett.* **2009**, *63*, 1471-1474.
5. Wetchakun, N.; Phanichphant, S. *Curr. Appl. Phys.* **2008**, *8*, 343-346.
6. Euvananont, C.; Junin, C.; Inpor, K.; Limthongkul, P.; Thanachayanont, C. *Ceram. Int.* **2008**, *34*, 1067-1071.
7. Nizard, H.; Kosinova, M. L.; Fainer, N. I.; Rumyantsev, Yu. M.; Ayupov, B. M.; Shubin, Yu. V. *Surf. Coat. Tech.* **2008**, *202*, 4076-4085.
8. Zhao, G.; Tian, Q.; Liu, Q.; Han, G. *Surf. Coat. Tech.* **2005**, *198*, 55-58.
9. Ghigna, P.; Speghini, A.; Bettinelli, M. *J. Solid State Chem.* **2007**, *180*, 3296-3301.
10. Arroyo, R.; Cordoba, G.; Padilla, J.; Lava, V. H. *Mater. Lett.* **2002**, *54*, 397-402.
11. Anpo, M.; Takeuchi, M. *J. Catal.* **2003**, *216*, 505-516.
12. Depero, L.; Sagaletti, L.; Allieri, B.; Bontempi, M.; Marino, L. E.; Zachii, M. *J. Cryst. Growth* **1999**, *198*, 516-520.
13. Kubacka, A.; Colón, G.; Fernández-García, M. *Catal. Today* **2009**, *143*, 286-292.
14. Kubacka, A.; Fernàndez-García, M.; Colón, G. *J. Catal.* **2008**, *254*, 272-284.
15. Zhu, J.; Chen, F.; Zhang, J.; Chen, H.; Anpo, M. *J. Photochem. Photobiol.* **2006**, *180*, 196-204.
16. Adán, C.; Bahamonde-Santos, A.; Fernández-García, M.; Martínez-Arias, A. *Appl. Catal. B* **2007**, *72*, 11-17.
17. Carnerio, J. O.; Teixeira, V.; Portinha, A.; Magalhaes, A.; Coutinho, P.; Tavares, C. J. et al. *Mater. Sci. Eng. B* **2007**, *138*, 144-150.
18. Colón, G.; Hidalgo, M. C.; Navío, J. A. *Appl. Catal. A Gen.* **2002**, *231*, 185-199.
19. Colón, G.; Maicu, M.; Hidalgo, M. C.; Navio, J. A. *Appl. Catal. B Environ.* **2006**, *67*, 41-51.
20. Rengaraj, S.; Venkataraj, S.; Yeon, J. W.; Kim, Y.; Li, X. Z.; Pang, G. K. H. *Appl. Catal. B Environ.* **2007**, *77*, 157-165.

21. Parida, K. M.; Sahu, N. *J. Mol. Catal. A Cheml.* **2008**, *287*, 151-158.
22. Burns, A.; Hayes, G.; Li, W.; Hirvonen, J.; Derek Demaree, J.; Ismat Shah, S. *Mater. Sci. Eng. B* **2004**, *111*, 150-155.
23. Guan, K.; Lu, B.; Yin, Y. *Surf. Coat. Tech.* **2003**, *173*, 219-223.
24. Guan, K. *Surf. Coat. Tech.* **2005**, *191*, 155-160.
25. Houmard, M.; Riassetto, D.; Roussel, F.; Bourgeors, A.; Berthome, G.; Joud, J. C. et al. *Appl. Surf. Sci.* **2007**, *254*, 1405-1414.
26. Enomoto, N.; Kawasaki, K.; Yoshida, M.; Li, X.; Uehara, M.; Hojo, J. *Solid State Ionics* **2002**, *151*, 171-175.
27. Liu, Z.; Zhang, X.; Murakami, T.; Fujishima, A. *Sol. Energy Mater. Sol. Cells* **2008**, *92*, 1434-1438.
28. Ye, X.; Zhou, Y.; Chen, J.; Sun, Y. *Mater. Chem. and Phys.* **2007**, *106*, 447-451.
29. Gao, W.; Chen, J.; Guan, X.; Jin, R.; Zhang, F.; Guan, N. *Catal. Today* **2004**, *93-95*, 333-339.
30. Zheng, M.; Gu, M.; Jin, Y.; Jin, G. *Mater. Sci. Eng. B* **2000**, *77*, 55-59.
31. Jiao, J.; Xu, Q.; Li, L. *J. Colloid Inter. Sci.* **2007**, *316*, 596-603.